Article

Magnetoswitchable Electrochemistry Gated by Alkyl-Chain-Functionalized Magnetic Nanoparticles: Control of Diffusional and Surface-Confined Electrochemical Processes

Eugenii Katz, Ronan Baron, and Itamar Willner

J. Am. Chem. Soc., **2005**, 127 (11), 4060-4070• DOI: 10.1021/ja042910c • Publication Date (Web): 25 February 2005

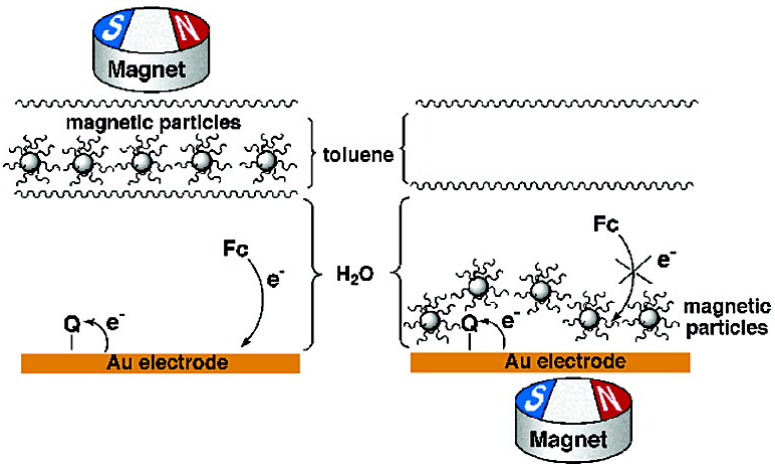

More About This Article

Additional resources and features associated with this article are available within the HTML version:

- Supporting Information
- Links to the 14 articles that cite this article, as of the time of this article download
- Access to high resolution figures
- Links to articles and content related to this article
- Copyright permission to reproduce figures and/or text from this article

View the Full Text HTML

J|A|C|S
ARTICLES
Published on Web 02/25/2005

Magnetoswitchable Electrochemistry Gated by Alkyl-Chain-Functionalized Magnetic Nanoparticles: Control of Diffusional and Surface-Confined Electrochemical Processes

Eugenii Katz, Ronan Baron, and Itamar Willner*

Contribution from the Institute of Chemistry, The Hebrew University of Jerusalem, Jerusalem 91940, Israel

Received November 24, 2004; E-mail: willnea@vms.huji.ac.il

Abstract: Magnetic nanoparticles consisting of undecanoate-capped magnetite (average diameter ca. 5 nm) are used to selectively gate diffusional and surface-confined electrochemical reactions. A two-phase system consisting of an aqueous buffer solution and a toluene phase that includes the suspended undecanoate-capped magnetic nanoparticles is used to control the interfacial properties of the electrode surface. Two different phenomena are controlled by attraction of the magnetic nanoparticles to the electrode by means of an external magnet: (i) The attracted magnetic nanoparticles form a hydrophobic layer on the electrode surface resulting in the blocking of diffusional electrochemical processes, while retaining the redox functions of surface-confined electrochemical units. (ii) For certain surface-immobilized redox species (e.g., quinones), the attraction of the magnetic nanoparticles to the electrode surface alters the mechanism of the process from an aqueous-type electrochemistry to a dry organic-phase-type electrochemistry. Also, bioelectrocatalytic and electrocatalytic transformations at the electrode are controlled by means of attraction of the magnetic nanoparticles to the electrode surface. Controlling the catalytic functions of the modified electrode by means of the magnetic nanoparticles attracted to the electrode is exemplified in two different directions: (i) Blocking of the bioelectrocatalyzed oxidation of glucose by glucose oxidase (GOx) using a surface-confined ferrocene monolayer as electron-transfer mediator. (ii) Activation of the microperoxidase-11 electrocatalyzed reduction of cumene hydroperoxide. In the latter system, the hydrophobic magnetic nanoparticles adsorb toluene, and the hydrophobic matrix acts as a carrier for cumene hydroperoxide to the electrode surface modified with the microperoxidase-11 catalyst.

Introduction

Monolayer-[1] or thin film-functionalized[2] electrodes are extensively used for controlling electrochemical transformations at the electrode surfaces. For example, the assembly of receptor-functionalized interfaces[3] or catalytic interfaces[4] were employed for the selective and sensitive electrochemical analysis of redox-active host substrates or for stimulating electrocatalytic processes at the conductive supports, respectively. Modification of electrode surfaces with densely packed long alkyl chains results in substantial blocking of the electron transfer between the redox species in solution and the conductive support.[5] Charged headgroups bound to monolayers[6] or thin films[7] associated with the electrodes provide selective discrimination of the redox species at the modified surfaces according to the charge of the species: The redox species of the same charge are repelled from the surface, and their electrochemical processes are inhibited,

(1) (a) Finklea, H. O. In *Electroanalytical Chemistry*; Bard, A. J., Rubinstein, I., Eds.; Marcel Dekker: New York, 1996; Vol. 19, pp 109−335. (b) Chechik, V.; Stirling, J. M. In *The Chemistry of Organic Derivatives of Gold and Silver*; Patai, S., Rappoport, Z., Eds.; Wiley: Chichester, 1999; Chapter 15, pp 551−640. (c) Ulman, A. *Chem. Rev.* **1996**, *96*, 1533−1554. (d) Delamarche, E.; Michel, B.; Biebuyck, H. A.; Gerber, C. *Adv. Mater.* **1996**, *8*, 719−729. (e) Bain, C. D.; Evall, J.; Whitesides, G. M. *J. Am. Chem. Soc.* **1989**, *111*, 7155−7164. (f) Bain, C. D.; Troughton, E. B.; Tao, Y.-T.; Evall, J.; Whitesides, G. M.; Nuzzo, R. G. *J. Am. Chem. Soc.* **1989**, *111*, 321−335.

(2) (a) Hillman, A. R. In *Electrochemical Science and Technology of Polymers*; Linford, R. G., Ed.; Elsevier: New York, 1987; Chapter 5, pp 103−239, Chapter 6, pp 241−291. (b) Chidsey, E. D.; Murray, R. W. *Science* **1986**, 231, 25−31. (c) Abruña, H. D. In *Electroresponse Molecular and Polymeric Systems*; Skotheim, T. A., Ed.; Marcel Dekker: New York, 1988; Vol. 1, 97−171.

(3) (a) Lahav, M.; Ranjit, K. T.; Katz, E.; Willner, I. *Israel J. Chem.* **1997**, *37*, 185−195. (b) Lahav, M.; Ranjit, K. T.; Katz, E.; Willner, I. *Chem. Commun.* **1997**, 259−260. (c) Kaifer, A. E. *Israel J. Chem.* **1996**, *36*, 389−397. (d) Flink, S.; van Veggel, F. C. J. M.; Reinhoudt, D. N. *Adv. Mater.* **2000**, *12*, 1315−1328. (e) de Jong, M. R.; Huskens, J.; Reinhoudt, D. N. *Chem. Eur. J.* **2001**, *7*, 4164−4170.

(4) (a) Murray, R. W. *Acc. Chem. Res.* **1980**, *13*, 135−141. (b) Murray, R. W.; Ewing, A. G.; Durst, R. A. *Anal. Chem.* **1987**, *59*, 379A−388A. (c) Abruña, H. D. *Coord. Chem. Rev.* **1988**, *86*, 135−189.

(5) (a) Finklea, H. O.; Avery, S.; Lynch, M.; Furtsch, T. *Langmuir* **1987**, *3*, 409−413. (b) Che, G.; Li, Z.; Zhang, H.; Cabrera, C. R. *J. Electroanal. Chem.* **1998**, *453*, 9−17. (c) Becka, A. M.; Miller, C. J. *J. Phys. Chem.* **1993**, *97*, 6233−6239. (d) Takehara, K.; Takemura, H. *Bull. Chem. Soc. Jpn.* **1995**, *68*, 1289−1296. (e) Nakashima, N.; Deguchi. Y. *Bull. Chem. Soc. Jpn.* **1997**, *70*, 767−770. (f) Krysinski, P.; Brzostowska-Smolska, M. *J. Electroanal. Chem.* **1997**, *424*, 1997. (g) Terrettaz, S.; Cheng, J.; Miller, C. J. *J. Am. Chem. Soc.* **1996**, *118*, 7857−7858. (h) Becka, A. M.; Miller, C. J. *J. Phys. Chem.* **1992**, *96*, 2657−2668.

(6) (a) Katz, E.; Schlereth, D. D.; Schmidt, H.-L. *J. Electroanal. Chem.* **1994**, *367*, 59−70. (b) Malem, F.; Mandler, D. *Anal. Chem.* **1993**, *65*, 37−41. (c) Takehara, K.; Takehara, H. *Bull. Chem. Soc. Jpn.* **1995**, *68*, 1289−1296. (d) Lion-Dagan, M.; Katz, E.; Willner, I. *J. Am. Chem. Soc.* **1994**, *116*, 7913−7914.

(7) (a) Pardo-Yissar, V.; Katz, E.; Lioubashevski, O.; Willner, I. *Langmuir* **2001**, *17*, 1110−1118. (b) Liu, Y.; Zhao, M.; Bergbreiter, D. E.; Crooks, R. M. *J. Am. Chem. Soc.* **1997**, *119*, 8720−8721.

10.1021/ja042910c CCC: $30.25

whereas oppositely charged redox species are concentrated at the modified surface, and their electrochemical processes are enhanced (Frumkin effect).[8] The charge-controlled gating of the electrochemical processes can be reversibly activated or deactivated by the formation of the charged and noncharged interfaces upon changing the pH value of the solution, that results in the protonation and deprotonation of the headgroups,[9] or by photochemical isomerization of the headgroups that yields the charged or neutral units.[10] The cyclic ON−OFF formation of the charged and neutral monolayers or thin films on electrode surfaces by the external stimuli (the change of pH value or light signal) allowed the generation of "command interfaces" that selectively enhance or inhibit electrochemical processes.[11] These command interfaces were applied to control bioelectrochemical and bioelectrocatalytic processes. For example, the electrochemical activation of cytochrome *c*[12] or the bioelectrocatalytic oxidation of glucose in the presence of glucose oxidase[13] were controlled by the reversible formation of charges on the modified electrode surfaces.

Chemically functionalized nanoparticles[14] can be associated with modified electrode surfaces and used to enhance electrochemical,[15] photoelectrochemical,[16] or bioelectrochemical processes.[17] For example, layered arrays of Au nanoparticles cross-linked by photosensitizer-electron acceptor units generated photocurrents that were controlled by the structure of the interface.[16] Functionalized semiconductor nanoparticles linked to electrodes by means of molecular[18] or supramolecular[19] monolayer structures revealed enhanced photoelectrochemical activities. Also, glucose oxidase (GOx) reconstituted on the flavin adenine dinucleotide (FAD)-functionalized Au nanoparticles (1.4 nm) self-assembled on a Au electrode has demonstrated an unprecedented high turnover number (5000 s^{-1}) for the electron transfer to the conductive support.[20] Magnetic particles (micro- and nanosizes) functionalized with redox units were used to reversibly activate electrocatalytic and bioelectrocatalytic processes by magneto-induced attraction and retraction of the active units to and from the electrode surface, respectively.[21]

Recently we reported on the reversible blocking of the electrochemical and bioelectrocatalytic processes at electrodes by attraction of the hydrophobically modified magnetic nanoparticles to the electrode surface.[22] The magnetic nanoparticles (average diameter 5 nm) modified with long alkyl chains form, upon their attraction to the electrode, a hydrophobic thin film on the conductive support. This thin film, formed on the electrode surface, results in a low capacitance of the double charged layer and complete blocking of diffusional electrochemical processes. Magnetic retraction of the modified magnetic nanoparticles regenerates a bare electrode surface, which allows the diffusional electrochemical process. Reversible retraction and attraction of the hydrophobic magnetic nanoparticles to or from the electrode surface provides a means to reversibly activate or deactivate the diffusional electrochemical processes. In the present study, we report on the effect of hydrophobic magnetic nanoparticles attracted to the electrode, by means of an external magnet, on the electrochemistry at redox monolayer-functionalized electrodes. The results demonstrate that: (i) The attraction of the hydrophobic magnetic nanoparticles to the redox monolayer-functionalized interface may separate diffusional and surface-confined electrochemical processes, (ii) upon the attraction of the hydrophobic nanoparticles to the redox monolayer-functionalized interface, the mechanism of the electrochemical process may be altered from the mechanism characteristic to an aqueous environment to the mechanism operative in a dry nonaqueous medium, and (iii) the attraction of the hydrophobic magnetic nanoparticles to the redox-functionalized interface may either prohibit electrocatalytic processes involving water-soluble substrates or induce electrocatalysis in the presence of hydrophobic, water-insoluble substrates.

Experimental Section

Chemicals and Materials. 2-Chloro-3-[2-(dimethylbutylammonium chloride)ethyl]amino-1,4-naphthoquinone (**8**) was synthesized and purified according to the published method.[23] *N*-(Ferrocenylmethyl)-aminohexanoic acid (**4**) was synthesized and purified as described before.[13] Undecanoic acid, microperoxidase-11 (**6**), GOx, (EC 1.1.3.4; type X-S from *Aspergillus niger*), β-D-glucose, ferrocene monocarboxylic acid (**9**), cumene hydroperoxide (**10**), cystamine (2,2′-diaminodiethyl disulfide) (**1**), 2,3-dichloro-1,4-naphthoquinone (**2**), 4-(2-hydroxyethyl)piperazine-1-ethanesulfonic acid sodium salt (HEPES), 1-ethyl-3-(3-dimethylaminopropyl)carbodiimide (EDC), and all other chemicals were purchased from Sigma or Aldrich and used without further purification. Magnetic nanoparticles Fe_3O_4 coated with undecanoic acid shell were synthesized according to the published procedure with the difference that only a single capping layer was generated on the surface of the nanoparticles.[24] Ultrapure water from NANOpure Diamond (Barnstead) source was used throughout all the experiments.

(8) Delahay, P. In *Double Layer and Electrode Kinetics. Advances in Electrochemistry and Electrochemical Engineering*; Delahay, P., Tobias, C. W., Eds.; Wiley-Interscience, New York, 1965; Ch. 3.
(9) (a) Bryant, M. A.; Crooks, R. M. *Langmuir* **1993**, *9*, 385−387. (b) Schweiss, R.; Werner, C.; Knoll, W. *J. Electroanal. Chem.* **2003**, *540*, 145−151. (c) Schweiss, R.; Welzel, P. B.; Werner, C.; Knoll, W. *Langmuir* **2001**, *17*, 4304−4311. (d) Creager, S. E.; Clarke, J. *Langmuir* **1994**, *10*, 3675−3683. (e) Katz, E.; Lion-Dagan, M.; Willner, I. *J. Electroanal. Chem.* **1996**, *408*, 107−112.
(10) (a) Katz, E.; Lion-Dagan, M.; Willner, I. *J. Electroanal. Chem.* **1995**, *382*, 25−31. (b) Katz, E.; Willner, I. *Electroanalysis* **1995**, *7*, 417−419.
(11) (a) Doron, A.; Katz, E.; Tao, G.; Willner, I. *Langmuir* **1997**, *13*, 1783−1790. (b) Katz, E.; Willner, B.; Willner, I. *Biosens. Bioelectron.* **1997**, *12*, 703−719. (c) Willner, I.; Doron, A.; Katz, E. *J. Phys. Org. Chem.* **1998**, *11*, 546−560.
(12) Willner, I.; Lion-Dagan, M.; Marx-Tibbon, S.; Katz, E. *J. Am. Chem. Soc.* **1995**, *117*, 6581−6592.
(13) Willner, I.; Doron, A.; Katz, E.; Levi, S.; Frank, A. J. *Langmuir* **1996**, *12*, 946−954.
(14) (a) Shipway, A. N.; Katz, E.; Willner, I. *ChemPhysChem* **2000**, *1*, 18−52. (b) Katz, E.; Willner, I. *Angew. Chem., Int. Ed.* **2004**, *43*, 6042−6108.
(15) (a) Shipway, A. N.; Willner, I. *Acc. Chem. Res.* **2001**, *34*, 421−432. (b) Shipway, A. N.; Lahav, M.; Willner, I. *Adv. Mater.* **2000**, *12*, 993−998. (c) Lahav, M.; Gabai, R.; Shipway, A. N.; Willner, I. *Chem. Commun.* **1999**, 1937−1938. (d) Lahav, M.; Shipway, A. N.; Willner, I. *J. Chem. Soc., Perkin Trans. 2* **1999**, 1925−1931. (e) Shipway, A. N.; Lahav, M.; Blonder, R.; Willner, I. *Chem. Mater.* **1999**, *11*, 13−15.
(16) (a) Lahav, M.; Heleg-Shabtai, V.; Wasserman, J.; Katz, E.; Willner, I.; Dürr, H.; Hu, Y. Z.; Bossmann, S. H. *J. Am. Chem. Soc.* **2000**, *122*, 11480−11487. (b) Lahav, M.; Gabriel, T.; Shipway, A. N.; Willner, I. *J. Am. Chem. Soc.* **1999**, *121*, 258−259.
(17) Katz, E.; Willner, I.; Wang, J. *Electroanalysis* **2004**, *16*, 19−44.
(18) (a) Sheeney-Haj-Ichia, L.; Pogorelova, S.; Gofer, Y.; Willner, I. *Adv. Funct. Mater.* **2004**, *14*, 416−424. (b) Sheeney-Haj-Ichia, L.; Wasserman, J.; Willner, I. *Adv. Mater.* **2002**, *14*, 1323−1326.
(19) Sheeney-Haj-Ichia, L.; Willner, I. *J. Phys. Chem. B* **2002**, *106*, 13094−13097.
(20) Xiao, Y.; Patolsky, F.; Katz, E.; Hainfeld, J. F.; Willner, I. *Science* **2003**, *299*, 1877−1881.
(21) (a) Hirsch, R.; Katz, E.; Willner, I. *J. Am. Chem. Soc.* **2000**, *122*, 12053−12054. (b) Katz, E.; Sheeney-Haj-Ichia, L.; Bückmann, A. F.; Willner, I. *Angew. Chem., Int. Ed.* **2002**, *41*, 1343−1346. (c) Katz, E.; Sheeney-Haj-Ichia, L.; Willner, I. *Chem. Eur. J.* **2002**, *8*, 4138−4148. (d) Willner, I.; Katz, E. *Angew. Chem., Int. Ed.* **2003**, *42*, 4576−4588.
(22) Katz, E.; Sheeney-Haj-Ichia, L.; Basnar, B.; Felner, I.; Willner, I. *Langmuir* **2004**, *20*, 9714−9719.
(23) (a) Calabrese, G. S.; Buchanan, R. W.; Wrighton, M. S. *J. Am. Chem. Soc.* **1983**, *105*, 5594−5600. (b) Katz, E.; Shkuropatov, A. Y.; Vagabova, O. I.; Shuvalov, V. A. *J. Electroanal. Chem.* **1989**, *260*, 53−62.
(24) Shen, L.; Laibinis, P. E.; Hatton, T. A. *Langmuir* **1999**, *15*, 447−453.

Scheme 1. Functionalization of the Au Electrode with the Quinone (**3**), the Ferrocene (**5**), and Microperoxidase-11 (**7**)

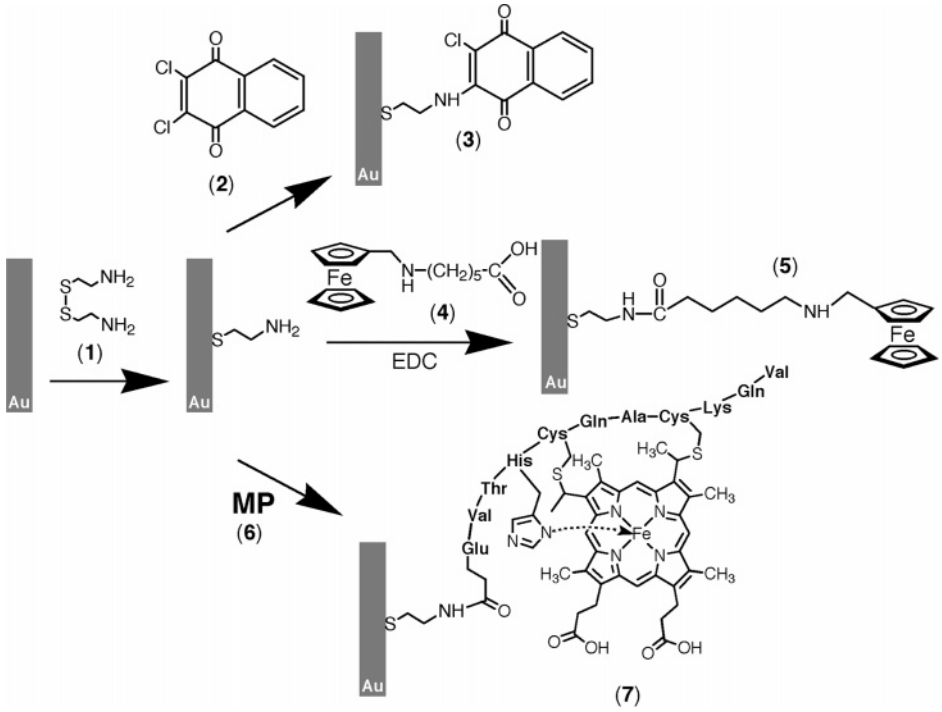

Chemical Modification of Electrodes. A Au-coated (50-nm gold layer) glass plate (Analytical-μSystem, Germany) was used as a working electrode. Cystamine (**1**) was self-assembled on the electrode as a monolayer to yield the amino-functionalized Au surface as described before.[25,26] The resulting amino-functionalized Au electrode was reacted with 2,3-dichloro-1,4-naphthoquinone (**2**) in boiling ethanolic solution for 3 min and thoroughly rinsed with ethanol and water to yield the amino-naphthoquinone monolayer (**3**) at a modified electrode as described before;[26] Scheme 1. Alternatively, the amino-functionalized Au electrode was reacted with *N*-(ferrocenylmethyl)aminohexanoic acid (**4**) (1 mM) in 0.1 M HEPES buffer, pH = 7.2, in the presence of EDC, 1 mM, for 2 h, to yield the ferrocene monolayer (**5**) on the Au electrode.[27] Similarly, the amino-functionalized Au electrode was reacted with microperoxidase-11 (**6**) (1 mM) in 0.1 M HEPES buffer, pH = 7.2, in the presence of EDC, 1 mM, for 2 h, to yield the microperoxidase-11 layer (**7**) on the Au electrode;[28] Scheme 1.

Electrochemical and Microgravimetric Measurements. Cyclic voltammetry measurements were performed using an electrochemical analyzer (model 6310, EG&G) connected to a personal computer with EG&G 270/250 software. The measurements were carried out at ambient temperature (25 ± 2 °C) in a conventional electrochemical cell consisting of a modified Au working electrode (0.3 cm^2 area exposed to the solution) assembled at the bottom of the electrochemical cell, a glassy carbon auxiliary electrode, and a saturated calomel electrode (SCE) connected to the working volume with a Luggin capillary. All potentials are reported with respect to this reference electrode. Phosphate buffer (0.1 M, pH 7.0) was used as a background electrolyte, unless stated otherwise. The undecanoic acid-functionalized magnetic nanoparticles were added to the cell in a toluene solution (0.5 mL, 1 mg mL^{-1}), yielding an upper organic solution layer immiscible with the aqueous electrolyte solution. The undecanoic acid-functionalized magnetic nanoparticles were attracted to the Au electrode surface from the upper organic layer by positioning a 12-mm diameter magnet (NdFeB/Zn-coated magnet with the remanent magnetization of 10.8 kG) below the bottom electrode. The magnetic nanoparticles were removed from the electrode surface and re-transported to the organic phase by positioning the external magnet on the top of the electrochemical cell. Argon bubbling was used to remove oxygen from the solutions in the electrochemical cell. The cell was placed in a grounded Faraday cage.

A QCM analyzer (Fluke 164T multifunction counter, 1.3 GHz, TCXO) and quartz crystals (AT-cut, 9 MHz, Seiko) sandwiched between two Au electrodes (area 0.196 cm^2, roughness factor ca. 3.2) were employed for the microgravimetric analyses in air.

Results and Discussion

The magnetic nanoparticles were prepared according to the literature procedure,[24] using undecanoic acid as a hydrophobic capping layer. The undecanoic acid-functionalized nanoparticles are freely suspendable in organic phases, such as toluene, and form a stable homogeneous suspension (a magnetic fluid[29]). TEM and AFM images of the nanoparticles indicated that the average diameter of the magnetic nanoparticles was ca. 5 nm.[22] The saturation magnetization of the nanoparticles at room temperature was determined to be ca. 36.4 emu g^{-1}.[22]

A biphase liquid system consisting of two immiscible solutions, aqueous and toluene, was placed in the electrochemical cell with a Au-plate working electrode located at the bottom. An aqueous buffer solution (2 mL; 0.1 M phosphate buffer, pH 7.0) was used as the background electrolyte, and the second toluene solution (0.5 mL) included the hydrophobic magnetic nanoparticles (1 mg mL^{-1}). As this organic phase is lighter than the aqueous phase, it is not in contact with the electrode surface at the bottom of the electrochemical cell. The hydrophobic

(25) (a) Katz, E.; Schlereth, D. D.; Schmidt, H.-L. *J. Electroanal. Chem.* **1994**, *367*, 59−70. (b) Katz, E.; Schlereth, D. D.; Schmidt, H.-L.; Olsthoorn, A. J. J. *J. Electroanal. Chem.* **1994**, *368*, 165−171.
(26) Katz, E.; Solov'ev, A. A. *J. Electroanal. Chem.* **1990**, *291*, 171−186.
(27) Blonder, R.; Katz, E.; Cohen, Y.; Itzhak, N.; Riklin, A.; Willner, I. *Anal. Chem.* **1996**, *68*, 3151−3157.
(28) Lötzbeyer, T.; Schuhmann, W.; Katz, E.; Schmidt, H.-L. *J. Electroanal. Chem.* **1994**, *377*, 291−294.
(29) (a) Berkovsky, B. M.; Medvedev, V. F.; Karkov, M. S. *Magnetic Fluids: Engineering Applications*; Oxford University Press: New York, 1993. (b) Rosensweig, R. R. *Ferrohydrodynamics*; Cambridge University Press: Cambridge, England, 1985.

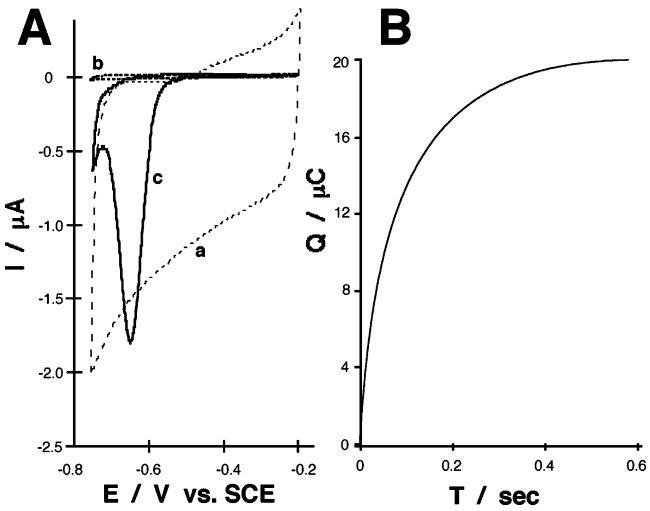

Figure 1. (A) Cyclic voltammograms measured at a Au electrode where (a) the magnetic nanoparticles are retracted from the electrode surface and located in the toluene phase, (b) the magnetic nanoparticles are attracted to the electrode surface from the toluene phase, and (c) the magnetic nanoparticles are attracted to the electrode surface from the toluene phase that includes the dissolved nitrobenzene, 2 mM. (B) Chronocoulometric transient measured upon the application of a potential step from −0.5 to −0.7 V in the presence of magnetic nanoparticles attracted to the electrode surface from the toluene phase containing nitrobenzene, 2 mM. The data were recorded using 0.1 phosphate buffer, pH 7.0, as an aqueous background electrolyte. Oxygen was removed from the solution by bubbling with Ar. Potential scan rate, 100 mV s^{-1}.

magnetic nanoparticles can be attracted to the working electrode by an external magnet placed below the electrode. The deposition of the magnetic nanoparticles on the electrode surface as a thin film turns the interface into a hydrophobic medium that blocks diffusional electrochemical reactions at the electrode surface and decreases the interfacial capacitance.[22] Figure 1A, curve a, shows a cyclic voltammogram of a bare Au electrode in 0.1 M phosphate buffer, pH 7.0, prior to the attraction of the hydrophobic magnetic nanoparticles. The cyclic voltammogram measured after the magnetic nanoparticles were attracted by the external magnet to the electrode surface shows significant decrease of the capacitance current; Figure 1A, curve b. This originates from the formation of a hydrophobic thin film composed of the hydrophobic magnetic particles and the entrapped toluene medium. To estimate the amount of the magnetic nanoparticles attracted to the electrode surface, the upper toluene layer containing the residual magnetic nanoparticles was collected and evaporated on a surface of a QCM electrode and the generated frequency change, $\Delta f = -880$ Hz, was measured in air. The mass of the magnetic nanoparticles, $\Delta m = 4.4$ μg, loaded on the QCM electrode and resulting in the frequency change was calculated using the Sauerbrey equation (eq 1), where f_0 is the base frequency of the crystal, ρ_q is the quartz density (2.648 g·cm^{-3}), μ_q is the shear modulus of the crystal (2.947 × 10^{11} dyn·cm^{-2} for AT-cut quartz), and A is the surface area:[30]

$$\Delta f = -2f_0\Delta m/A(\rho_q\mu_q)^{1/2} \quad (1)$$

The calculated mass corresponds to the magnetic nanoparticles remaining in the toluene phase after most of the nanoparticles were attracted to the bottom electrode by the external magnet. The residual amount of the nanoparticles in the toluene phase (4.4 μg) is only ca. 0.9% from the total amount of the nanoparticles (0.5 mg) introduced into the system. Therefore, most of the magnetic nanoparticles (ca. 495 μg, ca. 99.1%) were attracted to the electrode surface. Taking into account the average diameter of the nanoparticles (ca. 5 nm) and the density of the Fe_3O_4 core (ca. 5 g cm^{-3}), the number of the magnetic nanoparticles attracted to the electrode was estimated to be ca. 1.7 × 10^{15}. The number of the nanoparticles in a randomly densely packed single monolayer on the electrode surface (0.3 cm^2) was estimated to be ca. 1 × 10^{12}. Thus, the hydrophobic film generated on the electrode surface upon attraction of the magnetic nanoparticles is composed of ca. 1700 layers of the nanoparticles, and the average film thickness is ca. 8.5 μm.

To estimate the amount of the toluene associated with the hydrophobic magnetic nanoparticles, nitrobenzene, 2 mM, was added to the toluene solution as a redox label yielding a toluene/nitrobenzene molecular ratio that corresponds to 5 × 10^3. A cyclic voltammogram measured after the magnetic nanoparticles carrying toluene/nitrobenzene medium were attracted to the electrode surface shows an irreversible cathodic peak, $E_{pc} = -0.65$ V, corresponding to the reduction of nitrobenzene; Figure 1A, curve c. The charge associated with the reduction of nitrobenzene in the film (ca. 20 μC) was measured by chronocoulometry upon stepping the potential from −0.5 to −0.7 V; Figure 1B. The number of the nitrobenzene molecules, ca. 1.4 × 10^{14}, associated with the film generated on the surface was derived from the measured charge, assuming a one-electron reduction process in the nonaqueous medium.[31] Assuming that the toluene/nitrobenzene molecular ratio (5 × 10^3) in the film of the magnetic nanoparticles is the same as that in the bulk organic phase, one can estimate the number of the toluene molecules in the film to be ca. 0.7 × 10^{18}. Therefore, one magnetic nanoparticle is associated with ca. 410 toluene molecules.

Previous studies have shown that the formation of the hydrophobic film of the magnetic nanoparticles attracted to the electrode surface results in the blocking of diffusional electrochemical reactions.[22] Surface-confined redox species should be, however, still accessible to electrical contact, and thus, their electrochemical response should be observed in the presence of the magnetic nanoparticles on the electrode surface. Thus, the magneto-controlled deposition of the hydrophobic nanoparticles on modified electrode surfaces could, in principle, separate electrochemical processes of surface-confined redox units from the diffusional electrochemical processes of redox components solubilized in the electrolyte solution. To prove this concept, a monolayer of ferrocene (**5**) attached to a Au electrode was used as a surface-confined redox system, while quinone (**8**) dissolved in the aqueous background electrolyte, 2 × 10^{-4} M, was used as a diffusional redox component. The hydrophobic magnetic nanoparticles were dissolved in the toluene phase (1 mg mL^{-1}). As this organic phase is lighter than the aqueous phase, it is not in contact with the electrode surface. In this configuration, both electrochemical processes—the oxidation of the surface-confined ferrocene (**5**) and the reduction of the water-soluble quinone (**8**)—should be possible; Scheme 2A. The cyclic voltammogram of this system shows two reversible electro-

(30) Buttry, D. A.; Ward, M. D. *Chem. Rev.* **1992**, *92*, 1355−1379.

(31) Mann, C. K.; Barnes, K. K. *Electrochemical Reactions in Nonaqueous Systems*; Dekker: New York, 1970.

Scheme 2. Magneto-Controlled Reversible Translocation of the Hydrophobic Magnetic Nanoparticles between the Organic Phase and the Electrode Surface[a]

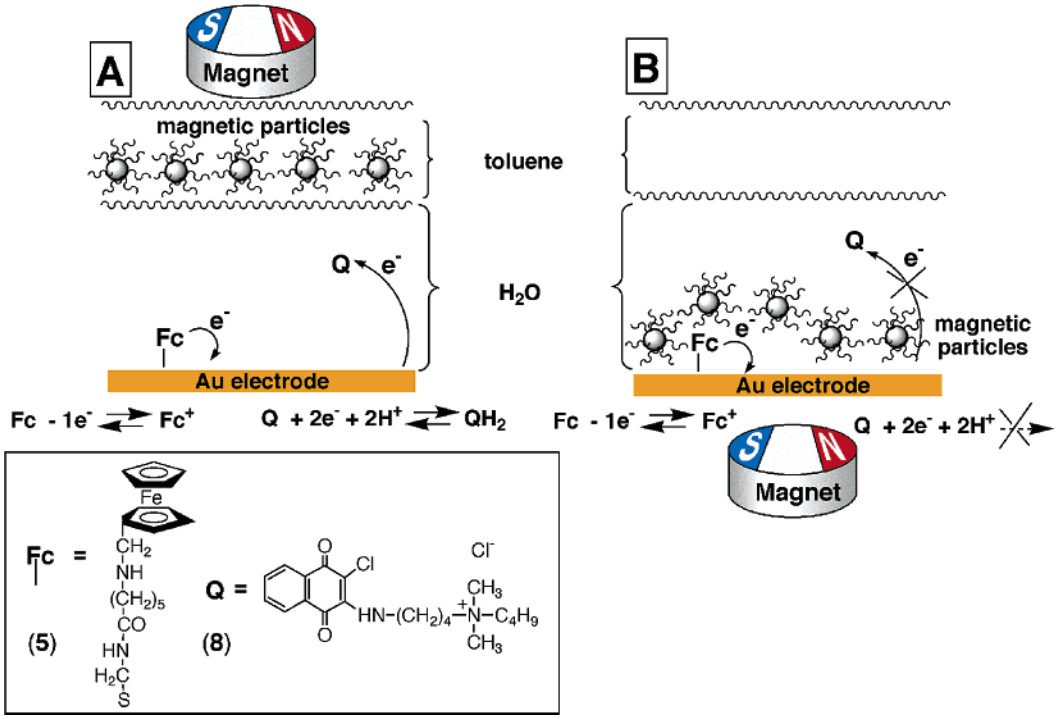

[a] (A) The magnetic nanoparticles are retracted from the electrode surface, and the electrode surface is electrochemically active for the diffusional process of the quinone (**8**) and for the surface-confined ferrocene (**5**). (B) The electrode surface is blocked by the hydrophobic magnetic nanoparticles attracted to the electrode by the external magnet toward the diffusional electrochemical process of the quinone (**8**) while retaining the surface-confined ferrocene (**5**) electrochemically active.

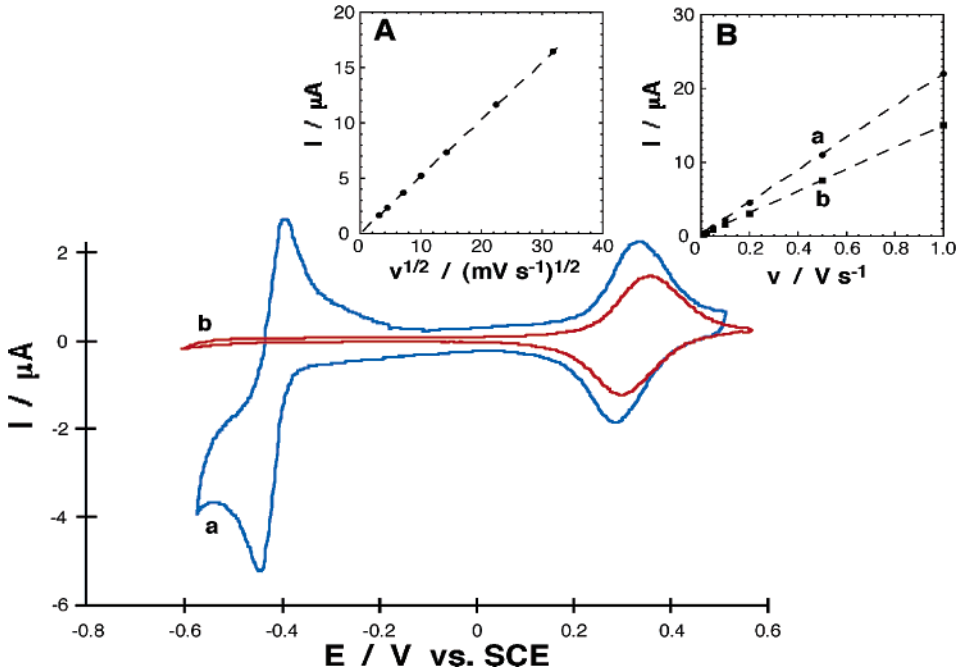

Figure 2. Cyclic voltammograms of the system consisting of a water-soluble quinone (**8**), 2×10^{-4} M, and surface-confined ferrocene (**5**) (a) when the hydrophobic magnetic nanoparticles are retracted from the electrode surface and (b) when the hydrophobic magnetic nanoparticles are attracted to the electrode surface. Insets: (A) The peak current dependence on the square root of the potential scan rate for the reduction of quinone (**8**). (B) The peak current dependence on the potential scan rate for the oxidation of ferrocene (**5**). (a) The magnetic nanoparticles are retracted from the electrode. (b) The magnetic nanoparticles are attracted to the electrode. Data were obtained at room temperature under Ar in a biphase system consisting of 0.1 M phosphate buffer, pH 7.0 (lower phase), and toluene with the magnetic nanoparticles, 0.5 mL, 1 mg mL^{-1} (upper phase). Potential scan rate 100 mV s^{-1}.

chemical processes at $E^\circ = -0.42$ V and $E^\circ = 0.32$ V, corresponding to the reduction of the quinone (**8**) and to the oxidation of the ferrocene (**5**), respectively; Figure 2, curve a. The diffusional character of the electrochemical process of the quinone (**8**) is obvious from the shape of the respective wave in the cyclic voltammogram. The diffusional redox mechanism of the quinone (**8**) is also proved by the fact that the peak current of the redox wave increases linearly with the square root of the

Scheme 3. Magneto-Controlled Reversible Translocation of the Hydrophobic Magnetic Nanoparticles between an Organic Phase, atop the Aqueous Electrolyte, and the Electrode Surface[a]

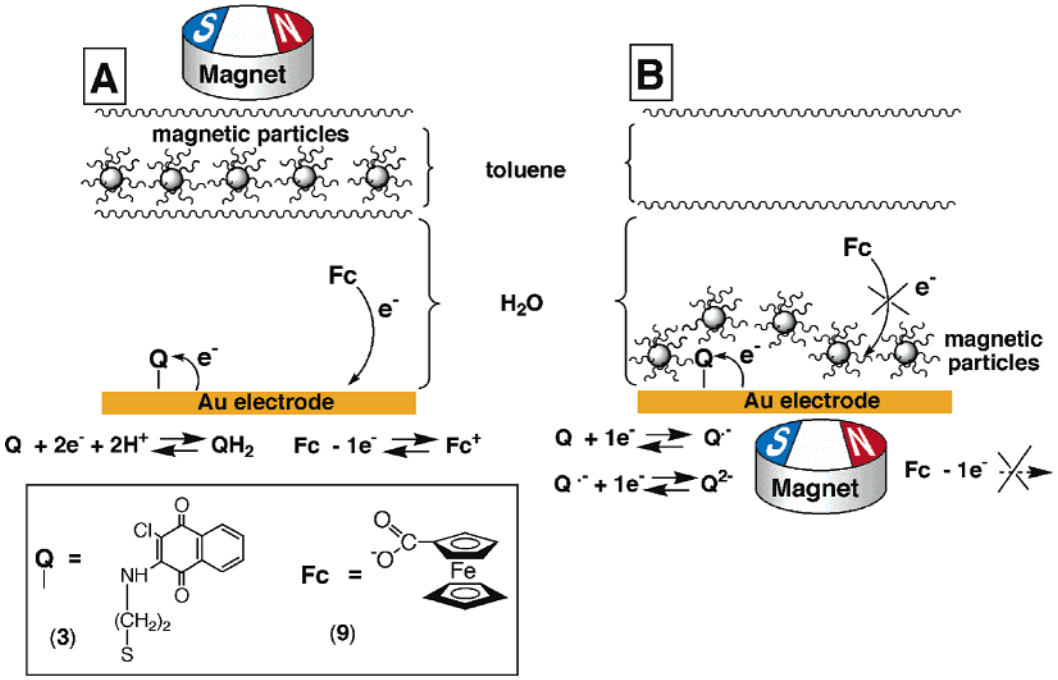

[a] (A) The magnetic nanoparticles are retracted from the electrode surface, and the electrode is activated toward the diffusional redox process of the ferrocene units (**9**) and toward the electrochemistry of the surface-confined quinone (**3**). (B) The electrode surface is blocked toward the diffusional electrochemical process of the ferrocene units (**9**) by the hydrophobic magnetic nanoparticles attracted to the electrode by the external magnet, while the surface-confined quinone (**3**) reveals nonaqueous-type electrochemistry.

potential scan rates; Figure 2, inset A.[32] The wave corresponding to the electrochemical process of ferrocene (**5**) has the shape characteristic to an electrochemical process of a surface-confined species. Also, the peak current of the ferrocene (**5**) oxidation wave relates linearly to the potential scan rate used in the cyclic voltammetry measurements (Figure 2, inset B, curve a), revealing the surface-confined character of the electrochemical process.[32] The surface coverage of the electrode with the ferrocene (**5**) units is ca. 7.7×10^{-11} mol cm^{-2}, according to the charge associated with the redox waves corresponding to the ferrocene units.

Positioning of an external magnet below the electrode attracts the hydrophobic magnetic nanoparticles to the electrode, and the interface is expected to be blocked toward the electrochemical process of the soluble quinone (**8**), but still to preserve the electrochemical activity of the surface-confined ferrocene (**5**); Scheme 2B. The cyclic voltammogram measured for this configuration shows, indeed, the complete blocking of the diffusional electrochemical process of the quinone units and a significant decrease of the capacitance current that originates from the formation of the hydrophobic thin film of the magnetic nanoparticles on the electrode surface; Figure 2, curve b. Nonetheless, the electrochemical wave corresponding to the ferrocene (**5**) units exists in the cyclic voltammogram, revealing that the hydrophobic thin film of the magnetic nanoparticles indeed separates the electrochemical process of the surface-confined redox species from the diffusional electrochemical reactions. The minor positive potential shift of the ferrocene (**5**) redox process, $E^\circ = 0.34$ V, originates from the change of the dielectric properties of the environment, similar to that reported for ferrocene monolayers diluted with hydrophobic alkyl chains of co-immobilized thiols.[1a,33] Also, the minute decrease of the number of the electrochemically accessible ferrocene (**5**) units, 6.2×10^{-11} mol cm^{-2}, reflected by a smaller charge associated with the electrochemical process in the presence of the magnetic nanoparticles, originates from the partial screening of the ferrocene (**5**) by the alkyl chains of the magnetic nanoparticles. This effect is also known for ferrocene units incorporated in monolayers of long alkyl thiols.[1a] The linear dependence of the peak current of the ferrocene (**5**) oxidation on the applied potential scan rate, in the system consisting of the magnetic nanoparticles attracted to the electrode, proves that the electrochemical process occurs on a surface-confined species; Figure 2, inset B, curve b. Positioning of the magnet above the cell retracts the hydrophobic magnetic nanoparticles from the electrode, resulting in the reactivation of the diffusional electrochemical process of the quinone (**8**); Scheme 2A. By the cyclic attraction of the hydrophobic magnetic nanoparticles to the electrode surface and their removal from the electrode support, by means of the external magnet, the diffusional electrochemical process of the quinone units is reversibly gated between "OFF" and "ON" states, respectively.

Another system that was examined to separate the electrochemical processes of a surface-confined redox species from a diffusional redox reaction, by means of the hydrophobic magnetic nanoparticles, is depicted in Scheme 3. As will be shown, the attraction of the hydrophobic magnetic nanoparticles to the electrode does not only lead to the blocking of the

(32) Bard, A. J.; Faulkner, L. R. *Electrochemical Methods: Fundamentals and Applications*; Wiley: New York, 1980.

(33) (a) Creager, S. E.; Rowe, G. K. *J. Electroanal. Chem.* **1997**, *420*, 291−299. (b) Andreu, R.; Calvente, J. J.; Fawcett, W. R.; Molero, M. *J. Phys. Chem. B* **1997**, *101*, 2884−2894. (c) Smalley, J. F.; Feldberg, S. W.; Chidsey, C. E. D.; Linford, M. R.; Newton, M. D.; Liu, Y. P. *J. Phys. Chem.* **1995**, *99*, 13141−13149.

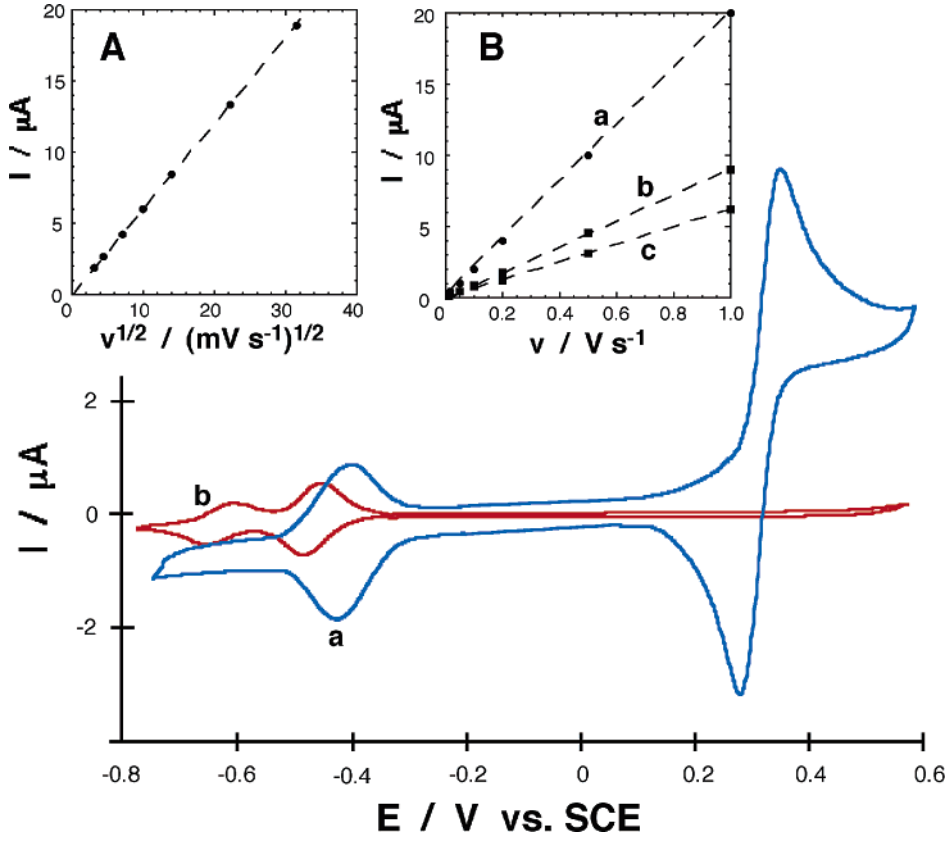

Figure 3. Cyclic voltammograms of the system consisting of the water-soluble ferrocene (**9**), 2×10^{-4} M, and the surface-confined quinone (**3**) (a) when the hydrophobic magnetic nanoparticles are retracted from the electrode surface and (b) when the hydrophobic magnetic nanoparticles are attracted to the electrode surface. Insets: (A) The peak current dependence on the square root of the potential scan rate for the oxidation of ferrocene (**9**). (B) The peak current dependence on the potential scan rate for the reduction of quinone (**3**). (a) The magnetic nanoparticles are retracted from the electrode. (b) The magnetic nanoparticles are attracted to the electrode (for the first cathodic peak, $E_1^\circ = -0.465$ V) (c) The magnetic nanoparticles are attracted to the electrode (for the second cathodic peak, $E_2^\circ = -0.630$ V). Data were recorded at room temperature under Ar in a biphase system composed of 0.1 M phosphate buffer, pH 7.0 (lower phase), and toluene with the magnetic nanoparticles, 0.5 mL, 1 mg mL^{-1} (upper phase). Potential scan rate 100 mV s^{-1}.

electrochemistry of the diffusional redox component, but it also alters the reaction mechanism of the surface-confined redox species due to the progress of the electrochemical process in a dry nonaqueous environment. The system is composed of a Au electrode surface modified with a monolayer of amino-naphthoquinone (**3**), and the water-soluble ferrocene monocarboxylic acid (**9**) was added to the aqueous electrolyte solution as the diffusional redox active component. Similarly to the previous system, the diffusional electrochemical oxidation of the ferrocene and the reduction of the surface-confined quinone units may proceed when the hydrophobic magnetic nanoparticles are retracted from the electrode surface; Scheme 3A. On the other hand, the attraction of the magnetic nanoparticles to the electrode surface is anticipated to block the diffusional process of the soluble ferrocene (**9**), while the electrochemical reduction of the quinone monolayer (**3**) in the hydrophobic environment provided by the nanoparticles is retained; Scheme 3B. The cyclic voltammogram of the system with the magnetic nanoparticles retracted from the electrode surface is depicted in Figure 3, curve a. It consists of a redox wave at $E^\circ = -0.41$ V corresponding to the reversible reduction of the quinone monolayer (**3**), 2.2×10^{-11} mol cm^{-2}, and an additional wave, $E^\circ = 0.33$ V, corresponding to the oxidation of the soluble ferrocene (**9**), 2×10^{-4} M. The diffusional character of the ferrocene redox process is evident from the linear dependence of the peak current on the square root of the potential scan rates used in cyclic voltammetry measurements; Figure 3, inset A. The surface-confined character of the electrochemical reaction corresponding to the quinone units is supported by the linear increase of the peak currents with the increase of the potential scan rates; Figure 3, inset B, curve a. When the hydrophobic magnetic nanoparticles are attracted to the electrode surface, the cyclic voltammogram shows, however, two waves corresponding to the electrochemical process of the immobilized quinone (**3**), $E_1^\circ = -0.465$ V; $E_2^\circ = -0.630$ V. Also, under these conditions the complete blocking of the diffusional electrochemical process of the water-soluble ferrocene (**9**) is evident, and a significant decrease in the capacitance current is observed. The peak currents of the quinone reduction waves increase linearly with the increased potential scan rate, indicating that the electron transfer occurs on a surface-confined species; Figure 3, inset B, curves b and c. It is well-known that in an aqueous medium the electrochemistry of quinones shows a single redox wave corresponding to the $(2e^- + 2H^+)$-electrochemical reduction, whereas in dry nonaqueous solutions (e.g., in acetonitrile, dichloromethane, or dimethylformamide) quinones show two consecutive redox waves corresponding to the $(1e^-)$-reduction steps each.[34] The addition of water to nonaqueous solvents (sometimes traces of water in nonaqueous solvents) results in the protonation of anionic reduced states of quinones, and it changes the electrochemical process of quinones typical to dry nonaqueous environment to the mechanism characteristic for

(34) Chambers, J. Q. In *The Chemistry of the Quinonoid Compounds*; Patai, S., Ed.; Interscience: New York, 1974; p 739.

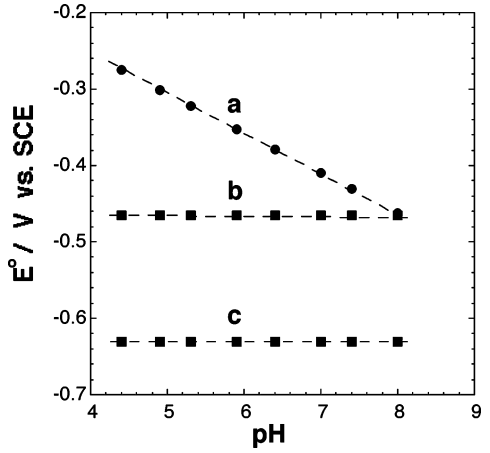

Figure 4. Dependence of the redox potentials, $E°$, of the immobilized quinone (**3**) on the pH value of the aqueous electrolyte solution (a) when the magnetic nanoparticles are retracted from the electrode surface, (b) when the magnetic nanoparticles are attracted to the electrode surface (the first step of the redox process, $E_1°$), and (c) when the magnetic nanoparticles are attracted to the electrode surface (the second step of the redox process, $E_2°$). Data were recorded at room temperature under Ar in a biphase system composed of 0.1 M Britton−Robinson buffer of variable pH values (lower phase) and toluene with the magnetic nanoparticles, 0.5 mL, 1 mg mL^{-1} (upper phase). Potential scan rate 100 mV s^{-1}.

aqueous solutions.[34] The two almost equal redox waves corresponding to the electrochemical process of the immobilized quinone (**3**), $E_1° = -0.465$ V; $E_2° = -0.630$ V, demonstrate that the attraction of the hydrophobic magnetic nanoparticles to the electrode surface provides a nonaqueous medium near the electrode surface, which is sufficiently dry to prevent protonation of the reduced anionic states of the quinone. The effective hydrophobic blocking of the electrode support by the functionalized magnetic nanoparticles is attributed to the partial carrying of toluene solvent by the hydrophobic nanoparticles. The coadsorbed toluene presumably forms a continued oil film that renders the interface into an organic-phase microenvironment, which acts as a barrier for proton transfer. The existence of an oil-like thin film adjacent to the electrode surface in the presence of the magnetically attracted nanoparticles will be further discussed by demonstrating that the film exhibits solubilization properties toward hydrophobic substances.

The redox potential of the quinone in the aqueous medium (when the magnetic nanoparticles are retracted from the electrode surface) depends on the pH value of the background electrolyte. Theoretically for a reversible ($2e^- + 2H^+$)-reduction process, the redox potential of the quinone units should be negatively shifted by 59 mV for the increase of each pH unit. We find that the shift of the redox potential of the immobilized quinone (**3**) is ca. 52 mV per a pH unit; Figure 4, curve a. The deviation of the experimental value of the slope, $\delta(E°)/\delta(\mathrm{pH})$, from the theoretical one was already observed in similar systems[26,35] and originates from the incomplete reversibility of the electrochemical process.[36] When the magnetic nanoparticles are attracted to the electrode surface, they generate a hydrophobic thin film, preventing the quinone monolayer from the contact with the aqueous bulk solution. The change of the pH value in the bulk electrolyte solution (using 0.1 M Britton−Robinson buffer with various pH values) does not affect the potentials of the two waves corresponding to the redox process of the quinone in the nonaqueous medium provided by the magnetic nanoparticles; Figure 4, curves b and c. Thus, the hydrophobic film generated by the magnetic nanoparticles prevents the protonation of the redox-active surface-confined species, and this leads to an electrochemical activity of the quinone units that is typical to a dry nonaqueous medium.

It is a common practice to activate soluble redox enzymes with electron-transfer mediator units bound to electrode surfaces.[37] Such systems represent good examples where the bioelectrocatalytic process includes diffusional steps as well as electrochemical reaction of surface-confined mediator units. Application of the hydrophobic magnetic nanoparticles allows the selective "ON" and "OFF" switching of the diffusional part of the process. We studied a bioelectrocatalytic system that included GOx and glucose as diffusional components and the ferrocene monolayer (**5**) confined to the electrode surface as an electron-mediating interface. When the magnetic nanoparticles are retracted from the electrode surface and upon application of a potential, which is positive enough to oxidize the ferrocene mediator ($E > 0.4$ V), the mediated bioelectrocatalytic oxidation of glucose by GOx should proceed in the system, and an electrocatalytic anodic current should be generated; Scheme 4A. Figure 5, curve a, shows the electrocatalytic current developed by the bioelectrocatalytic system. Upon the magnetic attraction of the nanoparticles to the electrode, they form a hydrophobic thin film that isolates the ferrocene-functionalized surface from the soluble enzyme/substrate system, resulting in the inhibition of the bioelectrocatalytic process; Scheme 4B. Figure 5, curve b, shows a cyclic voltammogram of the system upon attraction of the magnetic nanoparticles to the electrode. The cyclic voltammogram consists of the reversible redox process of the surface-confined ferrocene (**5**) units that are isolated by the magnetic nanoparticles from the aqueous bulk solution. Reversible magnetic retraction or attraction of the magnetic nanoparticles from or to the electrode surface, repeatedly, allows the cyclic activation or inhibition of the bioelectrocatalytic process; Figure 5, inset. That is, when the bioelectrocatalytic process is blocked by the magnetic nanoparticles attracted to the electrode surface, only the reversible redox process for the mediator is observed.

The previous system has demonstrated the use of the hydrophobic nanoparticles magnetically attracted to the electrode as a means to block interfacial bioelectrocatalytic processes. One may envisage, however, the design of an opposite system where the hydrophobic nanoparticles with coadsorbed toluene molecules carry a toluene-soluble substrate to the electrode surface upon the magnetic attraction of the nanoparticles to the electrode. As a result, in the presence of an appropriate surface-confined catalyst, electrochemical reduction (or oxidation) of the magnetically transported substrate may be activated. Toward this goal, microperoxidase-11 (**6**) was immobilized on the electrode surface, and cumene hydroperoxide (**10**) was dissolved in the toluene layer (2×10^{-3} M). Microperoxidase-11 immobilized on an electrode surface (**7**) is known to act as an electrocatalyst for the reduction of hydrogen peroxide in aqueous solutions[28] and of organic peroxides in nonaqueous solutions.[38]

(35) Katz, E.; Shkuropatov, A. Y.; Vagabova, O. I.; Shuvalov, V. A. *J. Electroanal. Chem.* **1989**, *260*, 53−62.
(36) Tarasevich, M. R.; Suslov, S. N.; Bogdanovskaya, V. A. *Sov. Electrochem.* **1984**, *20*, 1107−1115.
(37) Willner, I.; Katz, E. *Angew. Chem., Int. Ed.* **2000**, *39*, 1180−1218.
(38) Moore, A. N. J.; Katz, E.; Willner, I. *J. Electroanal. Chem.* **1996**, *417*, 189−192.

Scheme 4. Magneto-Controlled Reversible "ON"−"OFF" Switching of the Bioelectrocatalytic Oxidation of Glucose by GOx Using the Hydrophobic Magnetic Nanoparticles[a]

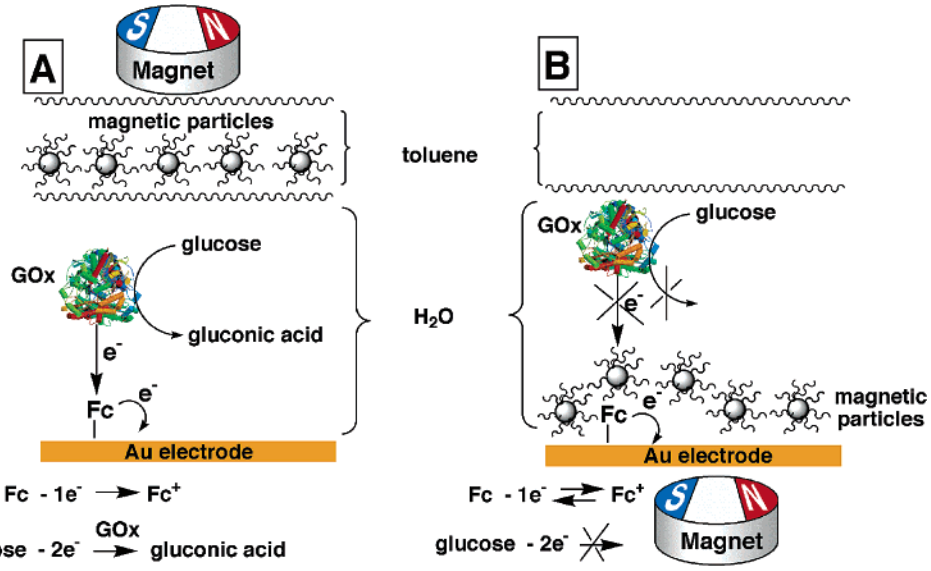

[a] (A) The magnetic nanoparticles are retracted from the electrode surface, which is activated toward the ferrocene-mediated bioelectrocatalytic oxidation of glucose. (B) The electrode surface is blocked by the hydrophobic magnetic nanoparticles toward the diffusional bioelectrocatalytic process, while the surface-confined ferrocene is electrochemically active.

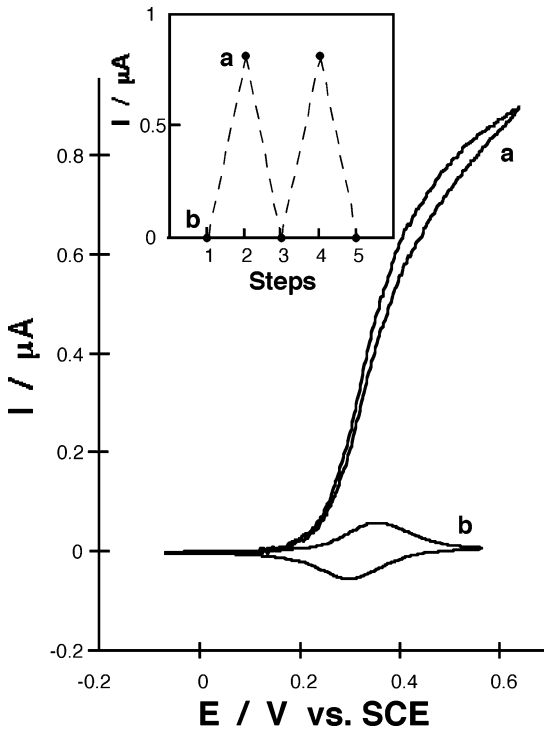

Figure 5. Cyclic voltamograms of the system consisting of the surface-confined ferrocene (**5**), glucose oxidase, 1 mg mL^{-1}, and glucose, 80 mM, dissolved in the aqueous phase (a) when the magnetic nanoparticles are retracted from the electrode surface and (b) when the magnetic nanoparticles are attracted to the electrode surface. Data were recorded at room temperature under Ar in a biphase system composed of 0.1 M phosphate buffer, pH 7.0 (lower phase), and toluene with the magnetic nanoparticles, 0.5 mL, 1 mg mL^{-1} (upper phase). Potential scan rate 5 mV s^{-1}. Inset: The reversible switch of the current generated by the system at $E = 0.5$ V. (a) The magnetic nanoparticles are retracted from the electrode surface. (b) The magnetic nanoparticles are attracted to the electrode surface.

Microperoxidase-11 was covalently bound through its carboxylic groups to the amino functions generated on a Au electrode surface by the self-assembly of cystamine. When the magnetic nanoparticles are retracted from the electrode surface, the microperoxidase-11-functionalized electrode surface is exposed to the aqueous environment (Scheme 5A), and a reversible redox process of the immobilized microperoxidase-11 can be observed (Figure 6A, curve a). Coulometric analysis of the redox wave indicates that the surface coverage of microperoxidase-11 is 1×10^{-10} mol cm^{-2}. When the hydrophobic magnetic nanoparticles are attracted to the electrode, they carry with the coadsorbed organic layer cumene hydroperoxide (**10**) to the microperoxidase-11-functionalized surface, thus providing the substrate for the bioelectrocatalytic reduction of cumene hydroperoxide (**10**) to the respective alcohol (**11**); Scheme 5B. Figure 6A, curve b, shows the cathodic electrocatalytic current in the presence of the magnetic nanoparticles carrying cumene hydroperoxide to the electrode surface. Reversible "ON" and "OFF" switching of the reduction of cumene hydroperoxide catalyzed by the immobilized microperoxidase-11 was accomplished upon cyclic attraction and retraction of the magnetic nanoparticles to and from the electrode surface, respectively; Figure 6A, inset. To find the amount of cumene hydroperoxide associated with the film, the charge corresponding to the reduction process was measured by chronocoulometry while applying a potential step from −0.2 to −0.7 V; Figure 6B. The charge associated with the complete reduction of cumene hydroperoxide in the thin film formed by the magnetic particles was found to be ca. 50 μC. Taking into account a two-electron reduction process for the peroxide,[39] we found that the respective amount of cumene hydroperoxide equals ca. 3×10^{-10} mol. The total volume of the film forming the magnetic nanoparticles was estimated to be ca. 2.6×10^{-4} cm^3 (taking into account the area of the electrode, 0.3 cm^2, and the film thickness, 8.5×10^{-4} cm). Nonetheless, in the randomly densely packed multilayer formed by the nanoparticles, about 60% of the volume is occupied by the nanoparticles and ca. 40% of the volume is filled with the accompanying toluene solvent and

(39) Baron, R.; Darchen, A.; Hauchard, D. *Electrochim. Acta* **2004**, *49*, 4841−4847.

Scheme 5. Magneto-Controlled Reversible "ON"−"OFF" Switching of Microperoxidase-11-Catalyzed Reduction of Cumene Hydroperoxide (**10**) by Means of the Hydrophobic Magnetic Nanoparticles[a]

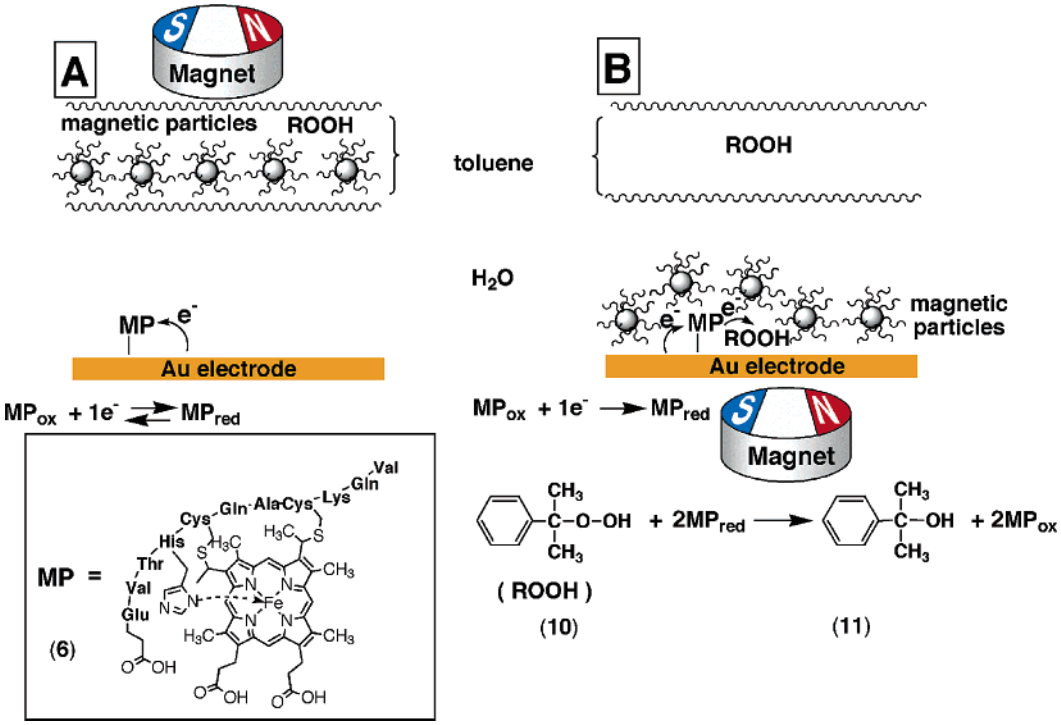

[a] (A) The magnetic nanoparticles are retracted from the electrode surface, and the immobilized microperoxidase-11 reveals a reversible redox process. (B) The hydrophobic magnetic nanoparticles with coadsorbed cumene hydroperoxide are attracted to the electrode by the external magnet, and the electrocatalytic reduction of cumene hydroperoxide by the immobilized microperoxidase-11 is stimulated.

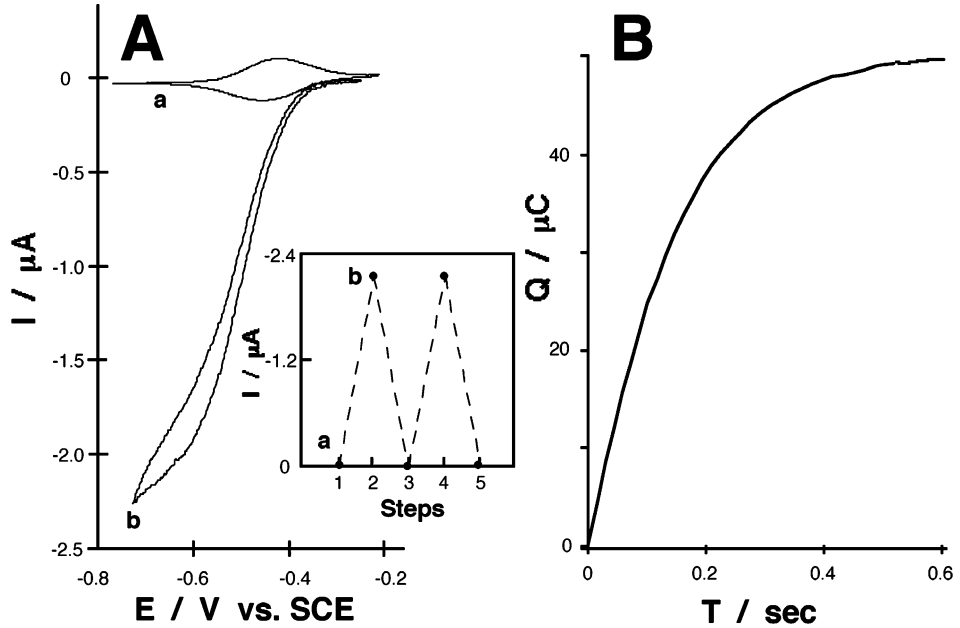

Figure 6. (A) Cyclic voltammograms of the system consisting of the surface-confined microperoxidase-11 (**7**) and cumene hydroperoxide (**10**), 2 mM, dissolved in the toluene layer (a) when the magnetic nanoparticles are retracted from the electrode surface and (b) when the magnetic nanoparticles are attracted to the electrode surface. Data were recorded at room temperature under Ar in a biphase system composed of 0.1 M phosphate buffer, pH 7.0 (lower phase), and toluene with the magnetic nanoparticles, 0.5 mL, 1 mg mL^{-1} (upper phase). Potential scan rate 5 mV s^{-1}. Inset: The reversible switch of the current generated by the system at $E = -0.7$ V. (a) The magnetic nanoparticles are retracted from the electrode surface. (b) The magnetic nanoparticles are attracted to the electrode surface. (B) Chronocoulometric transient measured upon the application of a potential step from −0.2 to −0.7 V in the presence of magnetic nanoparticles carrying cumene hydroperoxide and attracted to the electrode surface by the external magnet.

dissolved cumene hydroperoxide. Thus, the volume available in the film for cumene hydroperoxide can be estimated to be ca. 1×10^{-4} cm^3. Thus, the concentration of cumene hydroperoxide in the film is about 3 mM. This value is a factor of 1.5 higher than the bulk concentration of cumene hydroperoxide in the toluene phase. This could originate from the association of cumene hydroperoxide with the hydrophobic magnetic nanoparticles resulting in a 50% increase of the local concentration of cumene hydroperoxide in the organic shell around the nanoparticles.

Conclusions

The present study has described a new method to reversibly separate electrochemical processes of diffusional and of surface-confined redox species. When the hydrophobic magnetic nanoparticles are retracted from the electrode surface, both electrochemical processes (diffusional and surface-confined) can proceed. When the magnetic nanoparticles are attracted to the modified electrode surface, the diffusional electrochemical process is fully inhibited by the formation of a thin hydrophobic film on the electrode surface. In addition to the separation of the diffusional and surface-confined electrochemical processes, we demonstrated that the mechanism of the electrochemical process of a quinone-modified electrode could be altered from an aqueous-type redox process to an organic-phase mechanism upon the attraction of the magnetic nanoparticles to the electrode. The analysis of the latter results has implied that the assembly of the hydrophobic magnetic nanoparticles on the electrode surface yields an isolating thin film that prevents the transport of protons and water molecules to the electrode surface. This property was attributed to the coadsorption of toluene molecules to the hydrophobic nanoparticles that results in an impermeable thin film for H^+/H_2O on the electrode. A further topic that was addressed in the study has involved the use of the hydrophobic magnetic nanoparticles to control electrocatalytic transformations at electrode surfaces. Two configurations of such systems were discussed: In one configuration the bioelectrocatalytic oxidation of glucose was blocked by the attraction of the magnetic nanoparticles to the electrode, as a result of preventing the electrical contact between the solubilized GOx and the functionalized electrode. In the second configuration, the electrocatalyzed reduction of cumene hydroperoxide by the microperoxidase-11-functionalized electrode was stimulated by the attraction of the magnetic nanoparticles to the electrode surface. In this system, the electrocatalytic process is activated by carrying the water-insoluble substrate to the catalytic interface by means of the hydrophobic nanoparticles.

Acknowledgment. This research is supported by the EC MOLDYNLOGIC project.

JA042910C